Journal of

Applied and Computational Mechanics

Shahid Chamran
University of Ahvaz

Journal of Applied and Computational Mechanics

Numerical Investigation of Enhanced Oil Recovery from various Rocks by Nanosuspensions Flooding

D.V. Guzei[1,2], A.V. Minakov[1,2], M.I. Pryazhnikov[1,2] S.V. Ivanova[1]

[1] Siberian Federal University, Krasnoyarsk, Russia, 79 Svobodny pr., Krasnoyarsk, 660041, Russian Federation, Email: DGuzey@sfu-kras.ru

[2] Kutateladze Institute of Thermophysics, SB RAS, Novosibirsk, 630090, Russian Federation, Emails: AMinakov@sfu-kras.ru, MPryazhnikov@sfu-kras.ru, SVIvanova@sfu-kras.ru

Abstract. This work is devoted to the systematic numerical simulation of oil displacement using nanosuspension with silicon oxide particles with concentration of up to 1 wt% and particle sizes of 5 nm. The influence of such factors as core wettability, concentration of nanoparticles, capillary number, and oil viscosity on the enhanced oil recovery by nanosuspension has been systematically investigated using the VOF method for 2D-dimensional micromodels. Various rocks were considered: dolomite, metabasalt and sandstone. It is shown that the oil recovery coefficient improves for all considered types of rock with increasing nanoparticle concentration. The most effective application of nanosuspension for enhanced oil recovery is observed at a low capillary number, corresponding to the capillary displacement mode. The addition of nanoparticles facilitates increasing oil recovery factor in a wide range of viscosity ratios between oil and displacement fluid.

Keywords: Oil recovery factor, wettability, VOF method, numerical simulation, nanosuspension.

1. Introduction

The pursuit of developing radically new highly efficient and environmentally safe methods to intensify reservoir recovery prompts nanotechnology development. This line of development has great potential to improve methods of enhancing reservoir recovery and oil extraction mechanism [1-3]. These technologies are specific for the examined particles' size which is compatible with the radius of interphase interaction forces. This is important for the processes of oil displacement by nanosize objects, such as clays, aerosols, micellar colloidal solutions, polymer sols and gels, liquid films on the surface. Works of recent years shows that nanosuspensions make it possible to substantially enhance oil recovery factor (ORF) [1-8]. So, for example, a work [4] studies crude oil displacement with density of 0.86 g/cm^3 and viscosity coefficient of 11 cP from carbonate reservoir cores. The model of brine water was 5wt% sodium chloride solution. It formed the basis to prepare displacing nanosuspension adding SiO$_2$ particles in size of 20-70 nm and in concentration of 4 g/l into this solution. It was shown that the nanosuspension increased oil recovery up to 76%, while the oil recovery from waterflooding was 46%. Researchers note that this is due to the acquisition of the water-wetting properties by the rock, adsorbing the material and facilitates washing-out of both film and capillary confined oil. In the paper [5] heavy natural oil (density of 0.920 g/cm^3, and viscosity coefficient of 41 cP) was displaced by suspension of TiO$_2$ particles with diameter of 50 nm. Measurements show that nanofluid increased oil recovery factor minimum 1.3 times. Suleimanov et al. [6] used an aqueous solution of anionic surfactants with the addition of light metal nanoparticles as a flooding agent. It is shown that the use of such a nanofluid allowed reducing the surface tension at the oil boundary by 70–90% in comparison with an aqueous solution of a surface-active agent. At the same time, the volume of oil displaced by the nanofluid increased almost 1.5 times compared to the solution of anionic surfactant and 4.7 times compared to water.

After the advantages of nanosuspensions for enhanced oil recovery were demonstrated a large number of works appeared in which new nanomaterials were considered [7-8]. For example, Zhang et al. [7] used carbon nanosheets obtained from coal to enhance oil recovery. This allowed the oil/brine interfacial tension (IFT) to be reduced from 14.6 to 5.5 mN/m and increased oil recovery by 20%. In paper [8], a new nanosuspension was successfully developed based on functionalized nanocellulose. The influence of the injected volume, permeability and viscosity of oil on the efficiency of enhanced oil recovery with the flow of a nanosuspension was investigated. It is shown that the use of this suspension with nanocellulose provides an increase ORF by 3-17%. The search for new effective nanomaterials in order to enhance oil recovery has been continuing to this day.

Variable wettability of the rock providing variation of both capillary confined and film oil is among the reasons for the use surfactants in enhanced oil recovery methods. Addition of nanoparticles to the solutions can change the contact angle (CA) of wetting. In recent years numerous laboratory experiments showed high efficiency of nanoparticles to wettability alteration on the surface of different rock materials [9-13]. The conducted experiments showed that the wettability is not the only (and, probably, not the main one) performance indicator of nanoparticles with respect to washing the retained oil from rock.

Table 1. Density, viscosity coefficient and IFT of SiO2-nanosuspension at 25 °C.

NP, wt.%	Viscosity, mPa·s	Density, g/cm³	IFT, mN/m
0	0.8900	0.9970	22.3
0.125	0.8964	0.9977	21.5
0.25	0.8976	0.9984	21.2
0.5	0.9113	0.9997	20.4
1	0.9836	1.0025	21.9

Al-Anssari et al. [9] observed the increasing of nanoparticle concentration in order to decrease the contact angle of wetting; however, they recorded threshold values of 2 wt% SiO_2 above which the contact angle was not observed to change. The authors have come to a conclusion that the advanced fluids can change wettability of the calcite wetted by oil for strongly wetted by water; that being the case, the holding time plays a decisive role. Adsorption of nanoparticles also turned out to be irreversible. Alomair et al. [10] studied nanoparticles of 4 different materials and found a common trend in all materials. The interphase tension between heavy oil/advanced fluid decreases with an increase of nanoparticles concentration. The researchers [11] also obtained similar ratio of concentrations after studying the effect of Al_2O_3 and SiO_2 nanoparticles on mineral oil. In work [12] researchers confirmed that silicon nanoparticles do not significantly affect the interfacial tension. However, they point out that these nanoparticles can improve ORF by changing the wettability.

As can be seen from the review presented above, the main factors are the improvement of wettability and the decrease in interfacial tension. However, there is no consensus on the main mechanisms for enhancing oil recovery using nanosuspensions during reservoir flooding. Numerical modeling is required to establish the mechanisms of enhanced oil recovery, due to the fact that the physical processes are quite complex, and experimental studies are not enough.

This work is dedicated to the systematic numerical investigation of oil displacement using nanosuspension with silicon oxide particles. Influence of such factors as core wettability, concentration of nanoparticles, capillary number, and oil viscosity on the enhanced oil recovery by nanofluids was systematically investigated using the VOF method for 2D-dimensional micromodels. Unlike most of the well-known works on modeling the flows of nanofluids in porous media, in our work, for calculations, we used experimentally measured data on the properties of real nanofluids (contact angle, interfacial tension, viscosity, and density). For the first time, three different samples of real rock were examined: metabasalt, dolomite, and sandstone. There were no such complex computational and experimental studies before.

2. Experimental Investigation of the Suspensions Properties

Physical properties (viscosity, density, IFT and CA) of fluids are necessary for correct numerical simulation of the process of oil displacement from a porous medium. These properties have been measured experimentally. Nanosuspensions were prepared by a standard two-step method [13]. The nanosuspension preparation process is given in [14]. No surfactants were used. Nanosuspensions were prepared based on distilled water and powder of SiO_2 nanoparticles (NP) with average diameter 5 nm. The nanoparticle concentration varied from 0.125 to 1 wt%. Ultrasonic dispersant was used to break up particle agglomerates.

The physical properties of the nanosuspensions and oil are given in this subsection. The all properties measure at constant temperature of 25 °C.

Density and viscosity of oil is 0.831 g/cm³ and 7.8 mPa·s respectively. A detailed results description of experiments on the nanoparticles effect on wettability is presented in [15].

Measurement of IFT and CA was measured by means of tensiometer. Water and hexane were used to verify the surface tension coefficient measurement. Data variances did not exceed 5%. The absolute error in measuring the contact angle is 0.1°.

Brookfield viscometer was used to measure viscosity. The angular frequency of rotation of the measuring bob ranged from 1 to 200 rpm. Pycnometric method was used to estimate density. The uncertainty in determining the viscosity and density was about 2 and 1%, respectively.

Table 1 shows the physical properties of the nanosuspension (density, viscosity) and the nanosuspension-oil interfacial tension at different concentrations of SiO_2 nanoparticles (5 nm).
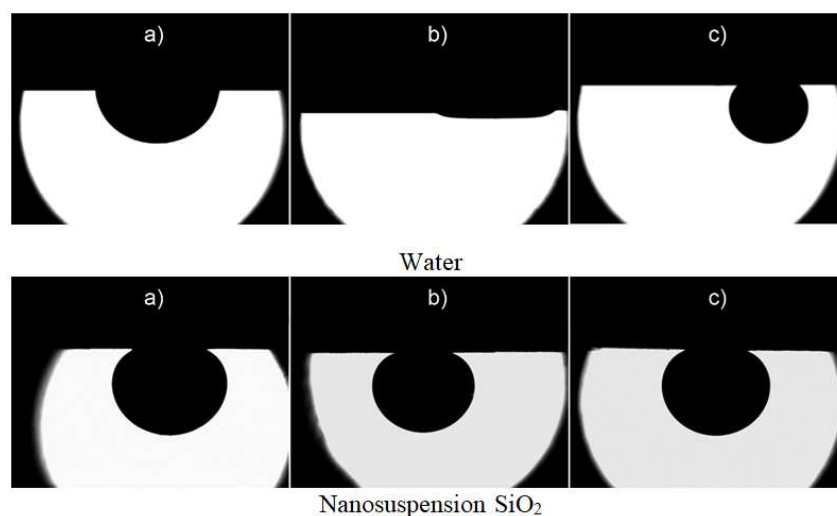
Fig. 1. Effect of the addition of SiO_2 nanoparticles (5nm, 1wt %) on the CA of the oil-rock-displacing fluid system. Rock: a) dolomite, b) metabasalt c) sandstone.
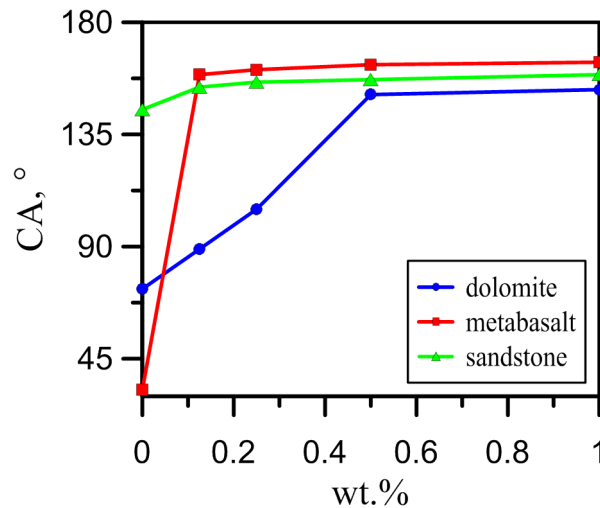
Fig. 2. The CA of nanosuspension-oil-rock vs. silicon concentration.

Further, the nanoparticles concentration effect on the oil wettability of the rock is considered. The three samples of rock were considered: metabasalt, dolomite and sandstone. Figure 1 (top row) shows a drop of oil in distilled water on these rocks. As can be seen, these rocks have very different wettability in the initial state. Metabasalt is hydrophobic and sandstone is hydrophilic. Dolomite has intermediate wettability. The nanoparticle additive radically changes the wettability of the rock with oil (see Fig. 1. bottom row). Metabasalt is most sensitive to the narticles addition. The contact angle of this material for the distilled water / oil system is about 33°, while for dolomite this angle is about 70°. Figure 2 shows the dependence of CA on nanoparticle concentration. Though initially the oil wetting of metabasalt was very good, the addition of nanoparticles to water radically degrades it. The nanoparticles effect on the CA on metabasalt is more significant. Therefore, while the addition of nanoparticles of 1 wt% increases the contact angle by 80° on dolomite at a SiO₂ concentration, this increase is about 130° on metabasalt. The effect of the nanoparticles addition is weaker on initially hydrophilic sandstone. Nevertheless, in this case, the nanoparticles addition leads to an increase in the contact angle by about 20°.

Thus, as a result of an experimental study, the effect of nanoparticles on the wettability alteration was shown. The IFT reduces with an increase in the nanoparticles concentration, while the CA for an oil drop in a nanosuspension on a rock, on the contrary, increases. This is very a significant influence (for example, from 33° to 160° for metabasalt). This means that the use of nanosuspensions can radically change the oil wettability of the rock, which makes it possible to significantly improve oil recovery by washout of the capillary-retained oil. The measured data were used in the numerical simulation.

3. Mathematical Model

The volume of fluid (VOF) method [16] was selected to simulate immiscible liquid-liquid flow in a porous medium. The VOF method uses a fixed computational grid and does not waste time on rebuilding the grid. Due to its effectiveness, this method has gained great popularity among researchers. This method has been repeatedly tested on a wide variety of problems and has shown good results [18-19]. The VOF method is conservative and maintains weight. The model can simulate two-phase flow by solving the momentum equation and using the displacement volume fraction α and the oil volume fraction ⍵. The sum of the volume fraction of oil and displacement fluid is 1.

The density and viscosity of the mixture is determined taking into account the volume fraction ⍵.

$$\rho = \rho_1(\varphi)\alpha + (1-\alpha)\rho_2 \tag{1}$$

$$\mu = \mu_1(\varphi)\alpha + (1-\alpha)\mu_2 \tag{2}$$

here ρ_2, μ_2 - density and viscosity of oil and $\rho_1(\varphi)$, $\mu_1(\varphi)$ - density and viscosity of nanosuspensions, which depend on NP concentration φ (see Table 1).

The conservation of mass:

$$\frac{dp}{dt} + \nabla\left(\rho \cdot \vec{V}\right) = 0. \tag{3}$$

Here $\vec{V}$ - mixture velocity.

Navier-Stokes momentum equation:

$$\frac{\partial}{\partial t}\left(\rho\vec{V}\right) + \nabla \cdot \left(\rho\vec{V}\vec{V}\right) = -\nabla p + \nabla \cdot \left[\mu\left(\nabla\vec{V} + \nabla\vec{V}^T\right)\right] + \vec{F}_s, \tag{4}$$

where p is static pressure of mixture, $\vec{F}_s$ is volume force vector.

The evolution of α is governed by the transport equation:

$$\frac{\partial \alpha}{\partial t} + \nabla \cdot \left(\alpha\vec{V}\right) = 0. \tag{5}$$

The continuum surface force algorithm proposed by Brackbill et al. [17] and taking into account capillary forces was used:

$$\vec{F}_s = \sigma(\varphi) k \nabla \alpha, \qquad (6)$$

where $\sigma(\varphi)$ is IFT, k is the curvature of the interface, which is determined as:

$$k = \nabla\left(\frac{\vec{n}}{|\vec{n}|}\right), \qquad (7)$$

where $\vec{n}$ is the normal vector, which is defined in the volume of the computational domain by the following equitation:

$$\vec{n} = \nabla \alpha. \qquad (8)$$

On the walls of the computational domain, the $\vec{n}$ is defined as follow:

$$\vec{n} = \vec{n}_w \cos(\theta(\varphi)) + \vec{\tau}_w \sin(\theta(\varphi)), \qquad (9)$$

here $\theta(\varphi)$ is CA at the wall, $\vec{n}_w$ is normal to the wall vector, $\vec{\tau}_w$ is tangential to the wall vector.

The measured data of physical properties (viscosity $\mu(\varphi)$, density $\rho(\varphi)$, IFT $\sigma(\varphi)$ and CA $\theta(\varphi)$) of nanosuspension were used. These data are given in section 2.

4. Numerical Techniques

A detailed numerical methodology is presented in [18-19]. The finite volume method is used for evaluating partial differential equations (3-5). The coupled between the pressure and velocity field is realized using the semi-implicit method for pressure linked equations-consistent (SIMPLEC) algorithm.

The SIMPLEC algorithm is a modification of a well-known in computational fluid dynamics SIMPLE algorithm. The algorithm follows the same steps like the SIMPLE algorithm. The difference between them is as follows. For SIMPLE algorithm, only the central coefficient in the coefficient matrix of the momentum equation is used in the flux correction expression. While SIMPLEC algorithm also uses the diagonal coefficients of the matrix of the momentum equation. The acceleration of the convergence of problems in which the relationship between velocity and pressure is an obstacle to obtaining a solution was observed using this modified correction equation. The algorithm allows using the relaxation parameter for the pressure equation equal to 0.8-0.9 instead of 0.2-0.3 for the SIMPLE algorithm. This gives an increase in the convergence rate by a factor of 1.6. In this case, the number of calculations at each iteration remains the same. This makes the SIMPLEC algorithm very efficient.

QUICK scheme was used to approximate convective terms of hydrodynamics equations.

The main limitation of the VOF method is the artificial blurring and deformation of the interface associated with numerical errors that arise when solving the transport equation. TVD with HRIC limiter was used to approximate the convective transport equation for VOF method. The using of this scheme can significantly improve the quality of solving the transport equation.

Source and diffusion flux terms were approximated by second order of accuracy. The Green-Gauss node based were selected for pressure gradient calculations and the momentum-continuity equations.

The staggered grids with PRESTO discretization scheme for pressure were used.

The time step corresponded to the condition the maximum of Courant–Friedrichs–Lewy number was equal to 2.

A 2D porous micromodel was used to study the process of oil displacement. The porosity of model was 40%. Permeability value for cores micromodel was 650 mD. The porous medium of the micromodel was obtained by randomly distributing circles with a diameter of 100µm (see Fig.3). The micromodel was a rectangle with a length and width of 5.3 and 1.875 mm respectively. The inlet boundary conditions were set with a fixed displacing fluid velocity, which corresponding to real conditions of core flooding. The outlet boundary conditions were set static pressure equal to zero. Symmetry conditions were established on the side walls.

At the initial moment of time, the entire pore space is filled with oil. The saturation of water at the initial time was zero in all calculations. In the process of displacing oil, the displacing fluid replaces the oil. The pressure drop in the micromodel and the oil recovery factor were determined. The ORF is defined as the ratio of the volume of displaced oil to the pore volume.

Three computational grids were used to evaluate the effect of mesh detail on the simulation result. The results of oil recovery factor (ORF) calculated for the base case are shown in Table 2. As you can see, the detailing of the grid of 350,000 cells is sufficient for obtaining an independent of further detailing solution. A computational grid consisting of 350,000 cells was used for further numerical simulation (see Fig. 4).

In addition, the described numerical algorithm and the numerical technique were previously tested by us on a large number of test problems of immiscible fluid flow in microchannels [19], as well as on the problem of oil displacement from a porous medium [20].
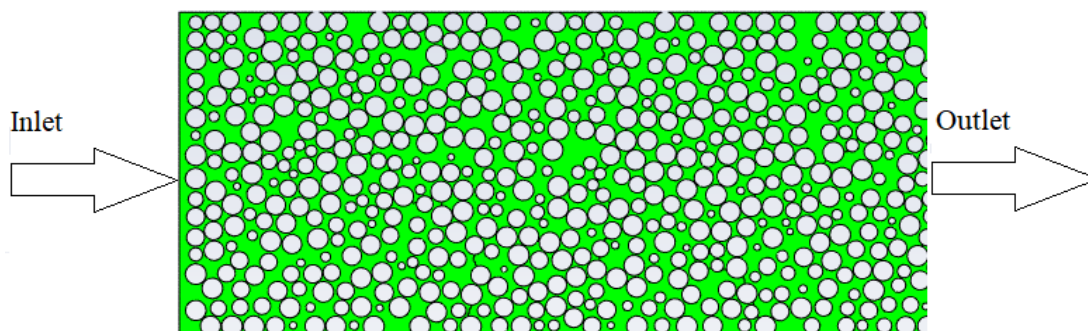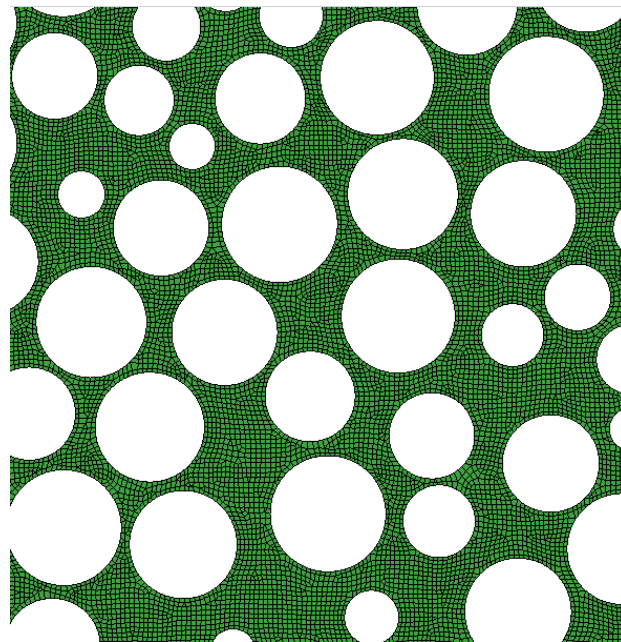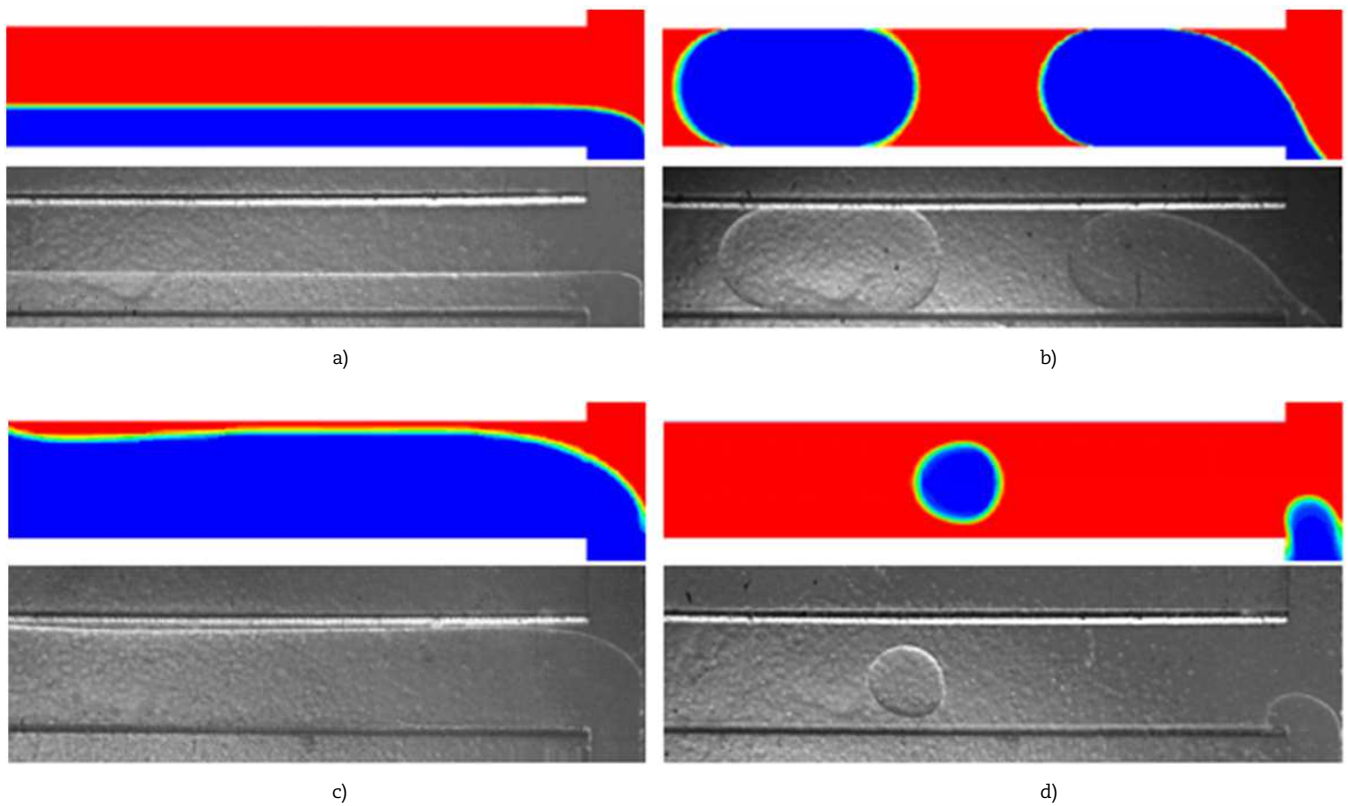

Fig. 3. Geometry of computational domain.

Table 2. Investigation of the computational grid detailing effect.

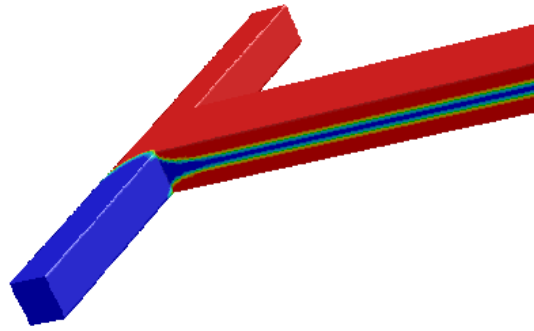| The grid cells number	ORF	Deviation in the most detailed mesh,%
175000	0.4115	6.3
350000	0.4300	1.8
1000000	0.4377	0

Fig. 4. The calculation mesh.

a)

b)

c)

d)

Fig. 5. A comparison of the calculation and experiment for different paraffin oil and castor oil flow modes in the microchannel: a) parallel mode; b) plug mode; c) slug mode; d) drip mode; e) rivulet mode.
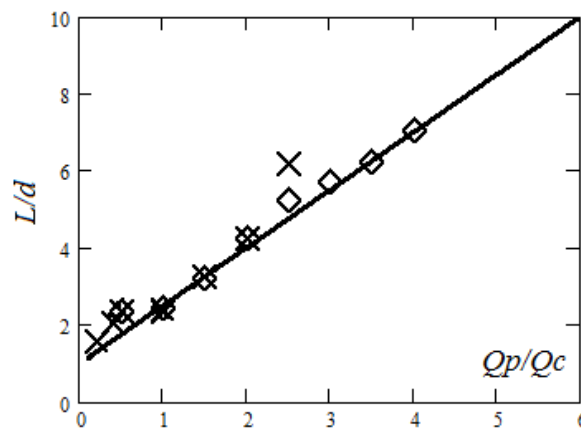
e)

Fig. 5. Continued.

Fig. 6. Dependence of the projectile dimensionless length on the ratio of the paraffinic and castor oils rates. Here: crosses show experimental data, rhombuses are calculated data.

5. Testing the Computational Algorithm

The described above mathematical model and numerical technique have been previously tested on a wide variety of test examples. The most typical example is presented there. The flow of two immiscible viscous liquids such as paraffinic and castor oils in a direct microchannel of a straight section was considered in that case [19]. The hydraulic channel diameter was 267 μm. The channel was made of SU-8 polymer. This provided good wetting of the channel walls with paraffin oil (contact angle 25°) and poor wetting with castor oil (contact angle 152°). The paraffin oil had a density of 845 kg/m^3 and a viscosity of 110 cps, while castor oil had a density of 935 kg/m^3 and a viscosity of 650 cps respectively. The flow of immiscible fluids in microchannels is of great importance in the problems of displacing oil from a porous medium because the efficiency of oil recovery significantly depends on the two-phase flow in the channels. The correctness of the algorithm reproducing all the regimes of immiscible fluid flow realized in the experiment is imperative. Therefore, this problem was chosen as a test in this work. A structured computational grid consisting of 800,000 cells was used. The computational grid cells were condensed to the walls of the computational domain. Running test calculations showed that the used computational grid is sufficient to obtain a reliable solution. A detailed study of the flow regimes of these fluids is given in our work [19]. The results showed that at given ranges of oil flow rates there were five different flow regimes in the microchannel: drip, plug, slug, rivulet and parallel. Typical flow regimes are shown in Fig. 5. A comparison of the calculated results (upper figures) with corresponding experimental photographs is given there. Rivulent flow is not visible in the photographs due to the strength of the flow. As can be seen, the used mathematical model and numerical technique are well reproducible in all cases for all flow regimes observed in the experiment. Apart from qualitative convergence, there is quantitative one between calculations and experiment results according to the phase interface and the most important forms of two-phase formation: their shape and size and the rate of formation, the shape and thickness of the liquid film, etc.

As an example, Fig. 6 shows a comparison between the estimated length of paraffin oil projectiles and experimental data. In the graph, the projectile length L is dimensioned for the hydraulic channel diameter d = 267 μm. As you can see, there is very good convergence. The size of the projectiles during the flow of immiscible fluids in microcavities is a very important factor since the efficiency of oil displacement during waterflooding largely depends on it. The calculation method reproduces this significant parameter.

In addition, the numerical technique was tested on a large number of various cases of two-phase and two-fluid flows in microchannels and porous media. Cases of gas projectiles movement in a rectangular minichannel are considered as well as cases of water and kerosene flow in a rectangular microchannel; cases of the gas-liquid flow in a T-shaped microchannel of circular cross-section; cases of modeling a stationary gas projectile in a minichannel; cases of modeling the formation of nitrogen bubbles in an aqueous solution of glycerin in an X-shaped microchannel. The results of this testing are published in our work [21]. The numerical results were compared with the data of known experiments. In all cases, good convergence between calculations and experiments was obtained. In our recent work [20], the problem of oil displacement from an inhomogeneous three-dimensional model of a porous medium was considered as a test. The simulation results were compared with the known experimental data from [22]. It is shown that the computational algorithm reproduces the data of the experiment obtained for the model sandstone according to residual oil saturation at different capillary numbers. This indicates the validity of this numerical technique applicability.
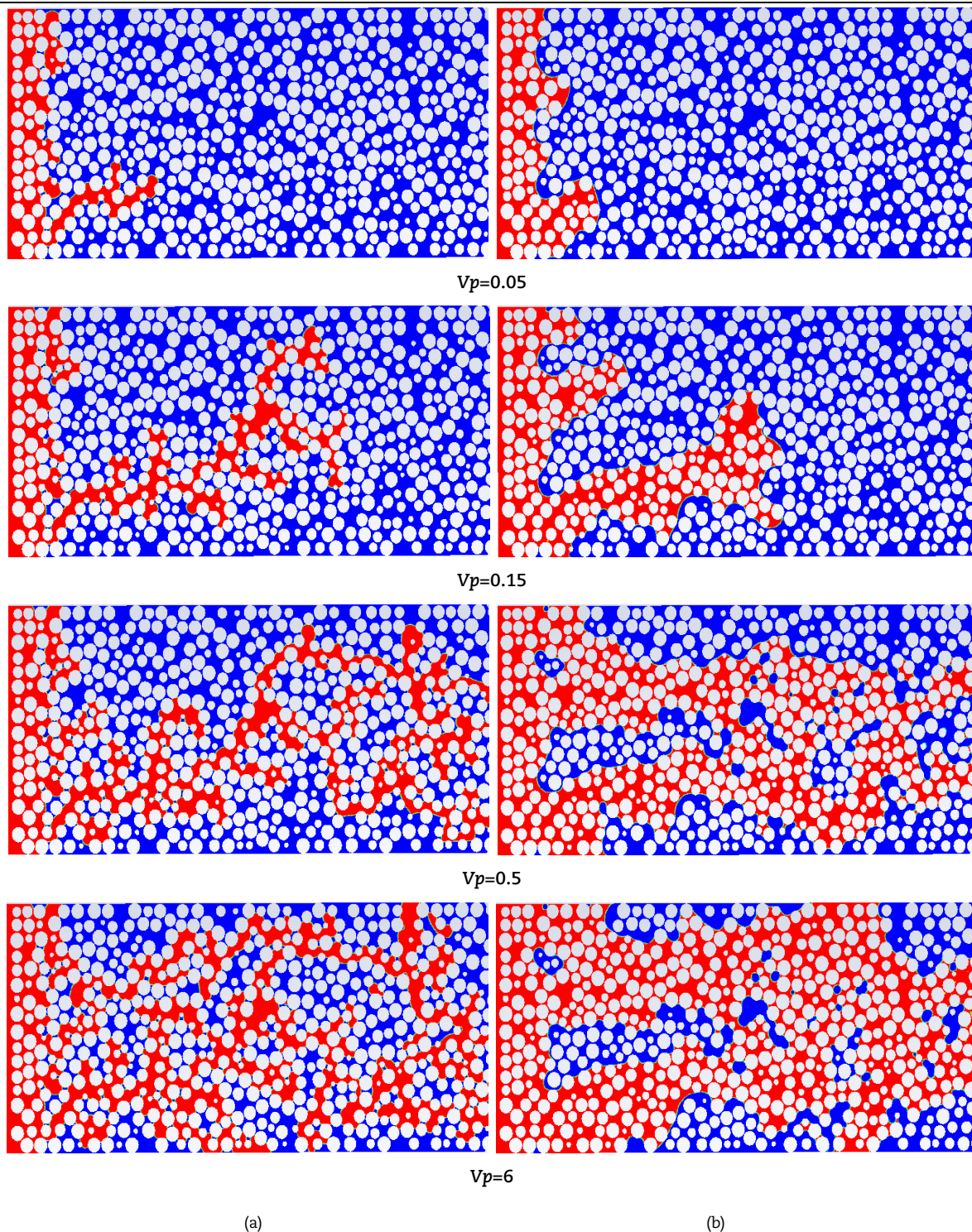
Vp=0.05

Vp=0.15

Vp=0.5

Vp=6

(a)   (b)

Fig. 7. Distribution of oil and displacing fluid during displacing by water (a) and nanosuspension (b) at different time moments.

6. Results of Numerical Research

6.1 Effect of capillary number on the displacement factor

Processes of oil displacement from the porous micromodel were numerically simulated for different capillary numbers. Water and water-based nanosuspension with silicon oxide (SiO$_2$) particles were considered for the calculations of displacing fluids. The rate values of displacing fluid at the micromodel inlet varied. Material of the porous medium was dolomite. The rate varied from 1×10^{-4} to 1×10^{-1} m/s. The range of rates corresponded to the capillary number values from 5×10^{-6} to 7.5×10^{-3}. The capillary number in the calculations was determined by the formula: $Ca = V\mu/\sigma$, where μ and σ are respectively the viscosity and the surface tension coefficient of the displacing liquid.
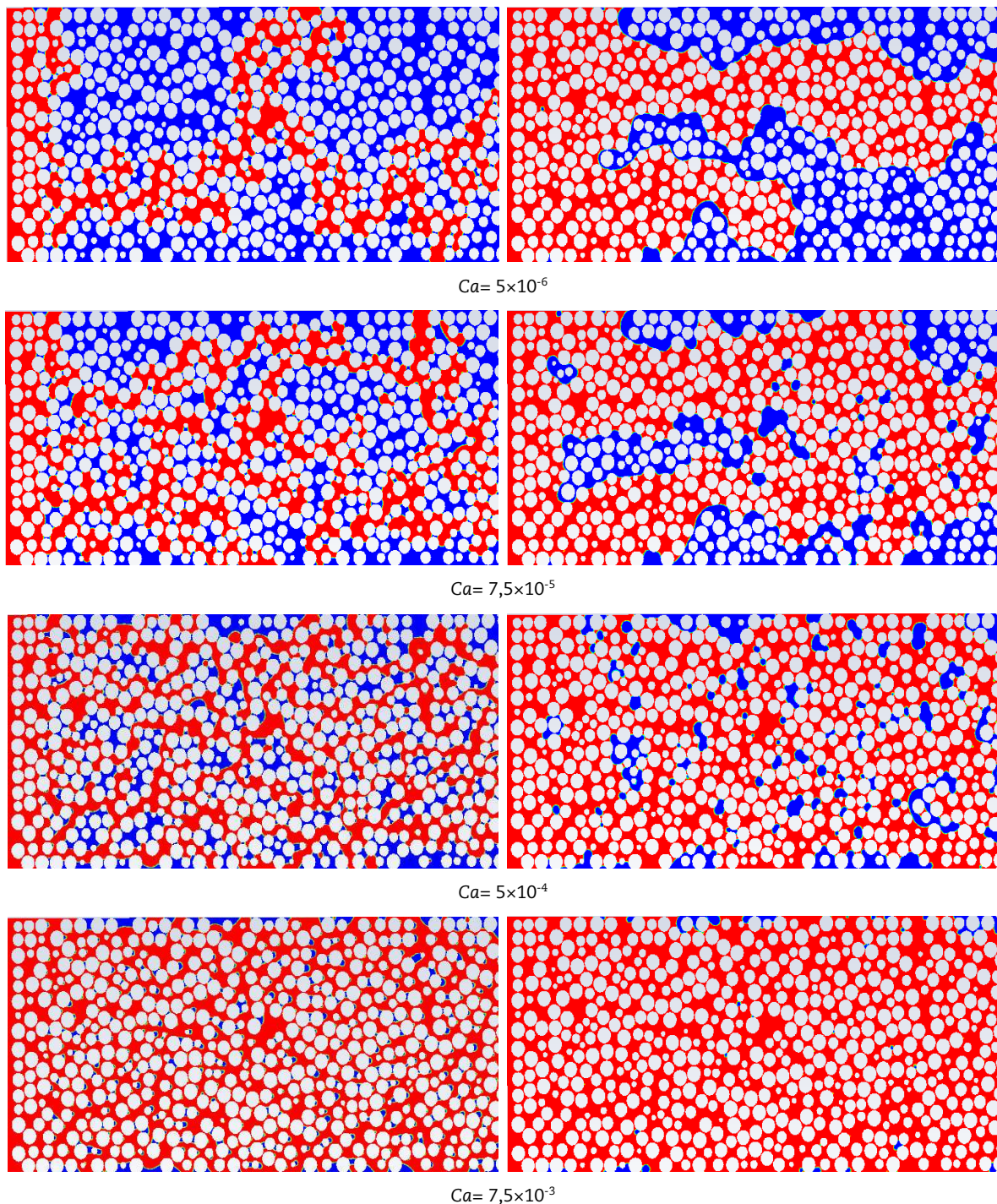
$Ca= 5\times10^{-6}$

$Ca= 7{,}5\times10^{-5}$

$Ca= 5\times10^{-4}$

$Ca= 7{,}5\times10^{-3}$

Fig. 8. Distribution of residual oil and displacing agent in micromodel for different capillary number values, left – water, right – nanosuspension, V_p=10.

Figure 8 shows patterns of oil distribution and displacing fluid in porous medium for different displacing fluid rates (V_P=10). On the left there are distribution patterns when the oil is displaced by water, on the right – displacement of oil by silicon oxide nanosuspension. As can be seen from Fig. 8, distribution of nanosuspension in the porous medium substantially differs from distribution of water. Nanosuspension as a displacing agent makes it possible to displace large amount of water from the porous medium – this is easy to see at the low rates of the displacing agent. We used dependences of ORF on the time of displacement and on the capillary number for quantitative characteristics. Dependences of oil recovery factor on time have been obtained for each calculation. Figure 9a shows a typical plot of this dependence. The oil recovery factor is shown to depend on time for water and silicon oxide nanosuspension for the rates of displacing agent at the entry equal to 1×10^{-3} and 1.5×10^{-2} m/s. From the plot shown in Fig. 9a it is seen that the ORF from the micromodel by nanosuspension is higher at the lower rates of displacing agent.

Fig. 7 shows the oil displacement process with time, (blue color is oil, and red color is the displacing fluid): water (a) and silicon oxide nanosuspension (b). The data on distribution have been obtained at a constant rate at the entry (1×10^{-3} m/s). Oil is displaced from the micromodel in different ways. Water breaks through the microporous model in separate thin jets leaving large regions filled with oil. Contrary to water the nanosuspension breaks though in broader jets, this leads to greater displacement of oil from the rock.
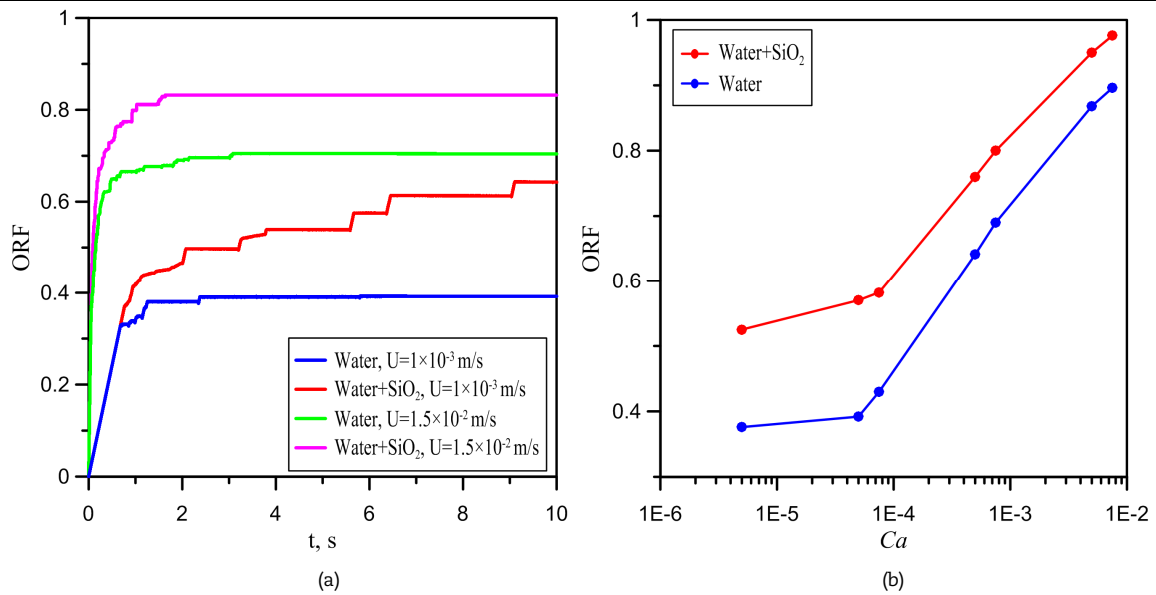
Fig. 9. Time dynamics of ORF (a) and dependence ORF on capillary number (b).
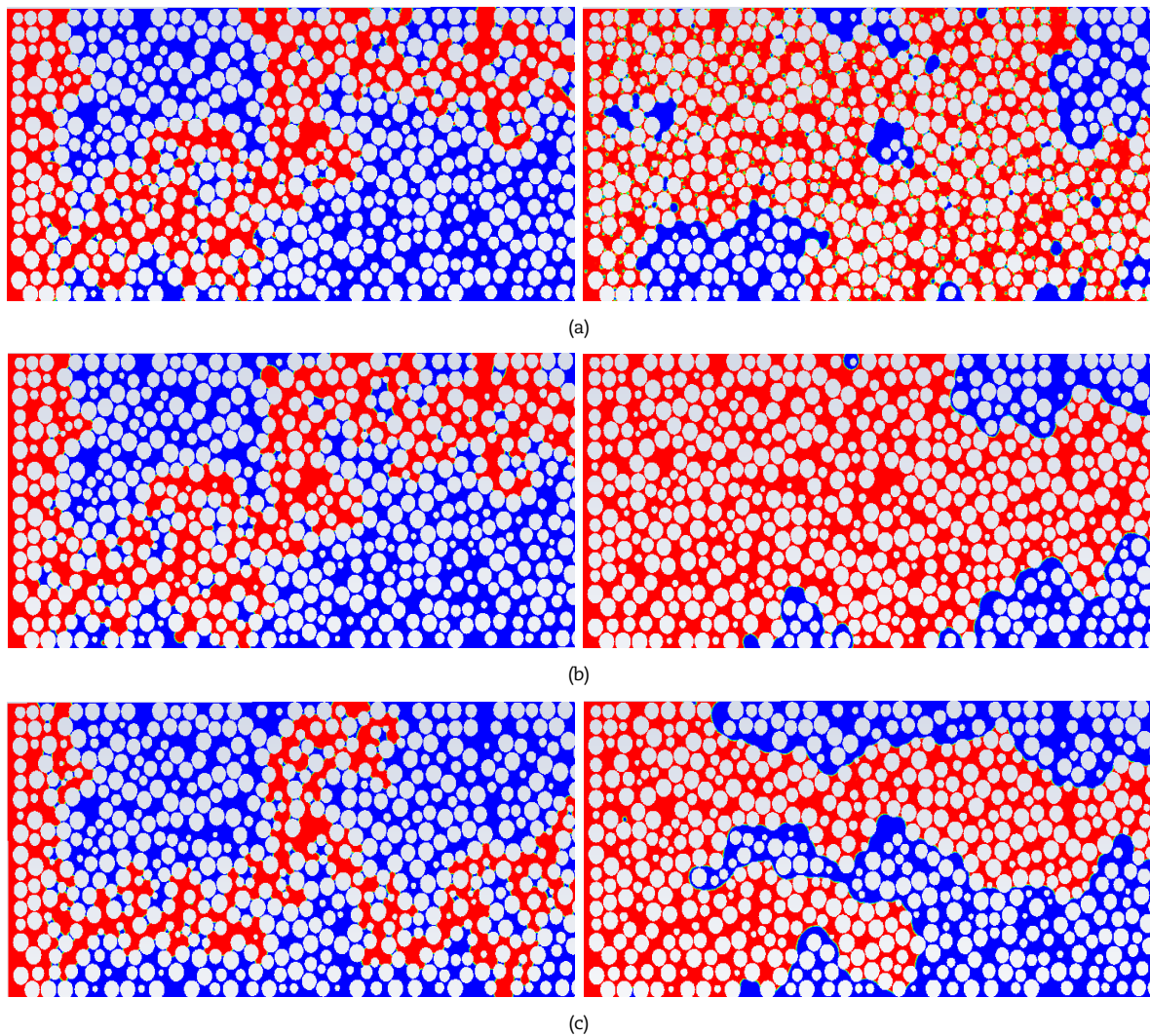

Fig. 10. Distribution of oil with different viscosity and displacing agent in porous medium left – water, right – nanosuspension, Vp=10.

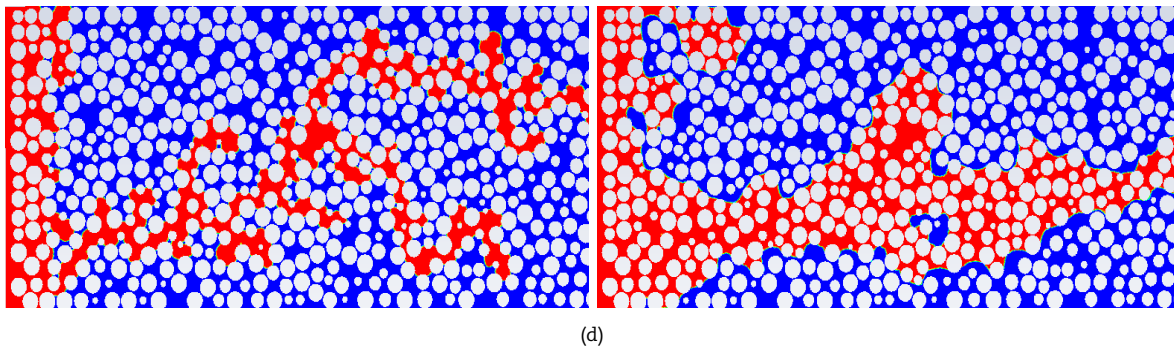a) $\mu_r = 1$; b) $\mu_r = 10$; c) $\mu_r = 40$; d) $\mu_r = 400$.
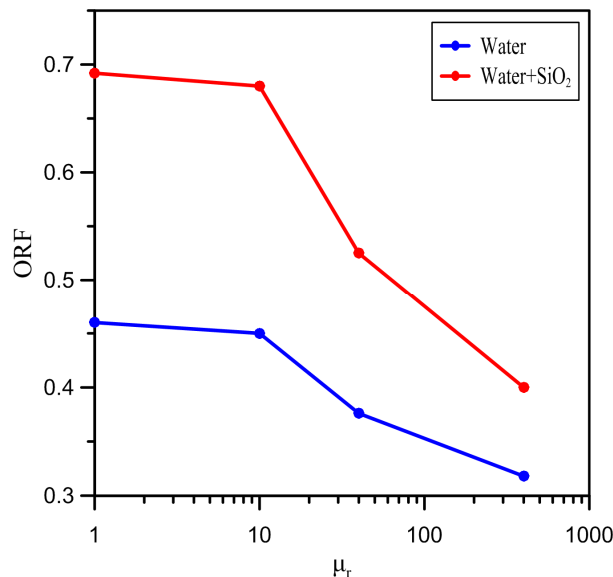
(d)

Fig. 10. Continued.

Fig. 11. Dependence of oil coefficient on relative viscosity for water and nanosuspension.

The influence of capillary number on oil recovery was carried out (see Fig. 9b). From the plot it is seen that the nanosuspension flooding to intensify the ORF over a broad range of capillary number values. The ORF is observed to be the most intensive at low Ca when the capillary forces prevail. E.g. at $Ca=5\times10^{-6}$ the use of nanosuspension provides an improve in the ORF by 40%. As the capillary number increase the intensification of oil recovery by nanosuspensions decreases. E.g. at $Ca=5\times10^{-4}$ the ORF by nanofluid flooding is 18% higher than by waterflooding.

6.2 Effect of oil viscosity on displacement factor

Oil displacement by water and nanosuspensions was numerically investigated with different values of oil viscosity coefficient. The studies have been carried out for the relative viscosity coefficient ($\mu_r = \mu_{oil} / \mu_{water}$) in the range of values from 1 to 400. The viscosity coefficient for water in the calculation was $\mu_{water} = 0.001$ Pa×s. This range of viscosities includes both low-viscosity oils and extremely high viscosity index oils. The rate of displacing agent at the entry into the computational domain was constant and equal to 1×10^{-4} m/s, this rate corresponds to the value of the capillary number $Ca=5\times10^{-6}$. The model used physical properties of SiO$_2$ suspension (1 wt%). The porous medium material in the calculations was dolomite.

Figure 10 shows distribution of residual oil and displacing fluid for different values of relative viscosity coefficient, $V_p=10$. The nanosuspension facilitates displacing larger amount of oil from the porous medium. Contrary to water which leaves large voids filled with oil after passage, the nanosuspension displaces oil from porous micromodel better. This is proved by quantitative analysis of numerical simulation results. Figure 11 shows dependence of oil recovery on relative viscosity. Application of nanosuspension allows to increase the ORF of low-viscosity oil by 50%. The coefficient of oil recovery by nanosuspension decreases to the oil recovery at water-flooding with an increase of the oil viscosity factor, but does not exceed the oil recovery at water-flooding by 40% with relative viscosity equal to 40 and by 12% at relative viscosity equal to 400. This gives a reason to conclude that the using of nanosuspension allows improving the oil recovery over a broad range of oil viscosities.

6.3 Oil displacement by nanosuspension in different rocks

Processes of oil displacement from porous media for different rock materials have been studied numerically. The calculations considered the following rock materials: dolomite, metabasalt, sandstone. The model used experimentally found values of contact angle for the rock under study and displacing fluid (water or nanosuspension). The influence of the nanoparticles concentration on CA for different rock materials is shown in Fig. 2. In the calculations the value of capillary number was fixed $Ca=5\times10^{-6}$. The constant value of rate 1×10^{-4} m/s was set at the entry into the computation domain. The value of oil viscosity coefficient in the calculation was 40 cP. Experimentally found values of viscosity coefficient and nanosuspensions density were used, the data are given in Table 1. Figure 12 presents final distribution of oil shown in red and displacing fluid; left – water, right - SiO$_2$ - nanosuspension for different materials of porous media.
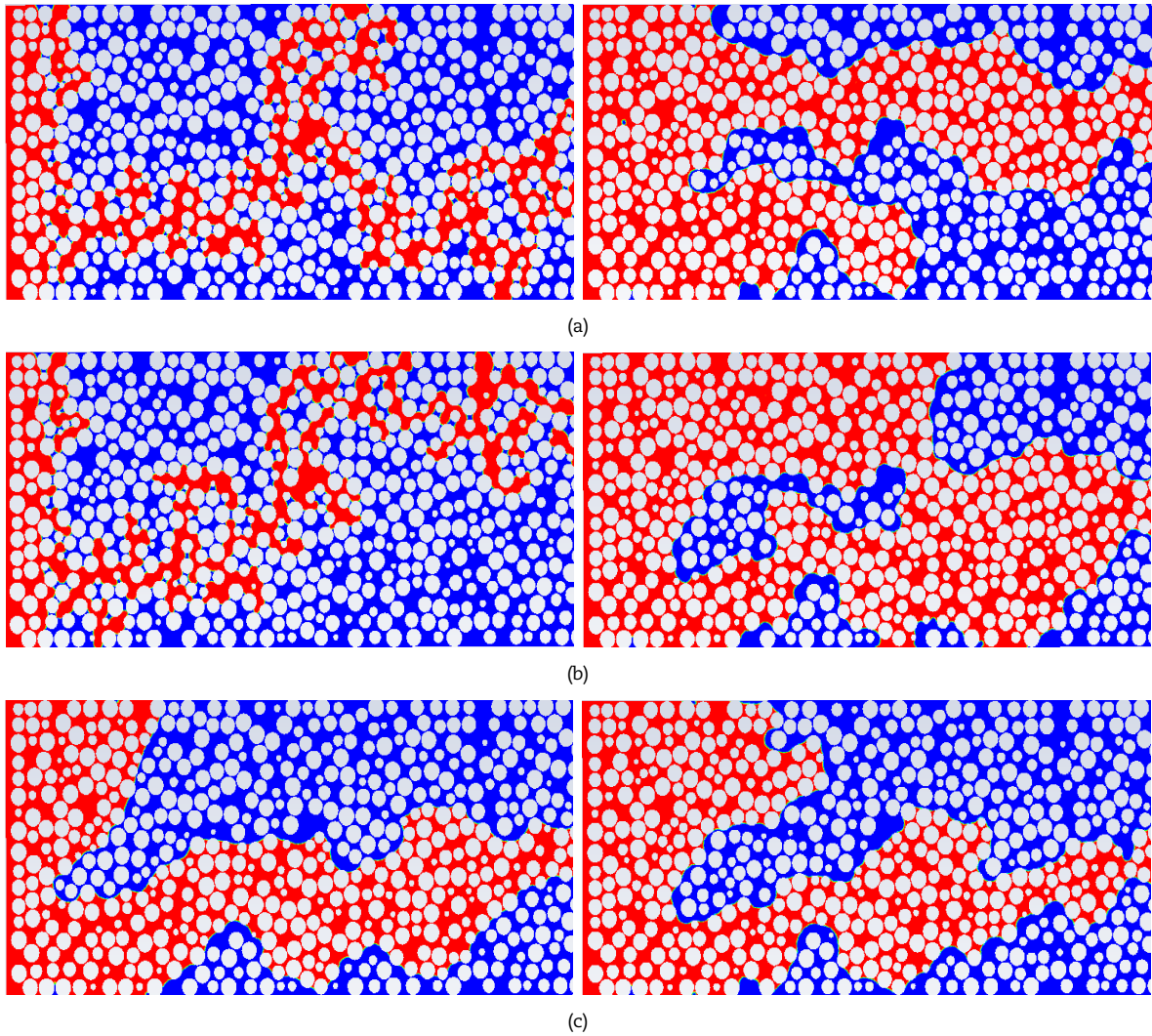
(a)

(b)

(c)

Fig. 12. Comparison of oil and displacing fluid distribution for different rock materials: a) dolomite; b) metabaslt, c) sandstone. Left – water, right - SiO$_2$ suspension., Vp=10.
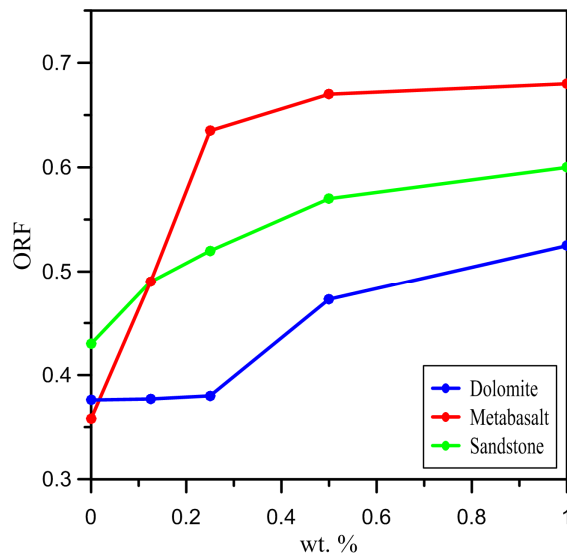

Fig. 13. Dependence of ORF on nanoparticles concentration for different rock materials.

Calculations produced dependences of oil recovery factor for different porous media materials during waterflooding and nanosuspension flooding were obtained. Figure 13 shows dependence of oil recovery factor on mass concentration of particles for different material of porous media. It can be seen from the plot in the figure that the oil recovery factor increases for all material of porous media under study with mass concentration. The factor of oil recovery by nanosuspension is the highest for metabasalt. The coefficient of oil recovery by nanosuspension for this rock material as a displacing agent with mass concentration of 1% is 89% higher than ORF by water. As for sandstone and dolomite the oil recovery factor values increase approximately by 39% when using 1% nanosuspension as compared to water.

7. Conclusion

The numerical investigation of the oil displacement process through porous micromodel with different wettability by SiO_2 nanosuspension has been conducted. Influence of such factors as core wettability, concentration of nanoparticles, capillary number, and oil viscosity on the enhanced oil recovery by nanosuspension has been systematically investigated using the VOF method for 2D-dimensional micromodels. Various rocks have been considered: dolomite, metabasalt and sandstone. The physical properties (density, viscosity, IFT and CA) were measured and used in a numerical study. The following results have been obtained:

1. It is shown that the oil recovery factor increases for all considered types of rock with increasing nanoparticle concentration. Especially the addition of nanoparticles significantly increases ORF for a hydrophobic rock. Therefore, the addition of nanoparticles increased the ORF by 89% for metabasalt.
2. The ORF for nanofluid increases for all types of rocks along with an increase in the capillary number. The most effective application of nanosuspension for enhanced oil recovery is observed at a low *Ca*, corresponding to the capillary displacement mode.
3. The addition of nanoparticles facilitates increasing ORF at different viscosity ratios between oil and displacement fluid. The effectiveness of using nanosuspensions in order to increase oil recovery is slightly reduced with an increase in oil viscosity for hydrophilic reservoirs.

Author Contributions

Guzei D.V. conducted numerical simulation and analyzed results, planned the scheme; Minakov A.V. developed the mathematical modeling and examined the theory validation; Pryazhnikov M.I. conducted the experiments and analyzed the empirical results; Ivanova S.V. conducted numerical simulation. The manuscript was written through the contribution of all authors. All authors discussed the results, reviewed, and approved the final version of the manuscript.

Acknowledgment

Funding

Not applicable.

Conflict of Interest

The authors declared no potential conflicts of interest concerning the research, authorship, and publication of this article.

Data Availability Statements

The datasets generated and/or analyzed during the current study are available from the corresponding author on reasonable request.

Nomenclature

μ	Viscosity [Pa·s]		V_p	Ratio of the volume of injected fluid to the pore volume
ρ	Density [kg/m³]		$\vec{V}$	Velocity vector
Ca	Capillary number		σ	Interfacial tension coefficient [N/m]

References

[1] Guo, K., Li, H., Yu, Z., Metallic nanoparticles for enhanced heavy oil recovery: promises and challenges, *Energy Procedia*, 75, 2015, 2068–2073.
[2] Liu, D., Zhang, X., Tian, F., Liu, X., Yuan, J., Huang, B., Review on nanoparticle-surfactant nanofluids: formula fabrication and applications in enhanced oil recovery, *Journal of Dispersion Science and Technology*, 2020, DOI:10.1080/01932691.2020.1844745.
[3] Sun, Y., Yang, D., Shi, L., Wu, H., Cao, Y., He, Y., Xie, T., Properties of Nano-fluids and Their Applications in Enhanced Oil Recovery: a Comprehensive Review, *Energy & Fuels*, 34(2), 2020, 1202-1218.
[4] Roustaei, A., Bagherzadeh, H., Experimental investigation of SiO_2 nanoparticles on enhanced oil recovery of carbonate reservoirs, *Journal of Petroleum Exploration and Production Technology*, 5, 2015, 27–33.
[5] Ehtesabi, H., Ahadian, M.M., Taghikhani, V., Enhanced Heavy Oil Recovery Using TiO_2 Nanoparticles: Investigation of Deposition during Transport in Core Plug, *Energy and Fuels*, 29(1), 2015, 1-8.
[6] Suleimanov, B.A., Ismailov, F.S., Veliyev, E.F., Nanofluid for enhanced oil recovery, *Journal of Petroleum Science and Engineering*, 78, 2011, 431-437.
[7] Zhang, B., Mohamed, A.I.A., Goual, L., Piri, M., Pore-scale experimental investigation of oil recovery enhancement in oil-wet carbonates using carbonaceous nanofluids, *Scientific Reports,* 10, 2020, 17539.
[8] Wei, B., Qinzhi, L., Wang, Y., Gao, K., Pu, W., Sun, L., An experimental study of enhanced oil recovery EOR using a greennano-suspension, *SPE Improved Oil Recovery Conference,* Tulsa, Oklahoma, USA, 2018.
[9] Al-Anssari, S., Nwidee, L.N., Ali, M., Sangwai, J.S., Wang, S., Barifcani, A., Iglauer, S., Retention of silica nanoparticles in limestone porous media, *Soc. Pet. Eng. - SPE/IATMI Asia Pacific Oil Gas Conf. Exhib.*, 2017.
[10] Alomair, O.A., Matar, K.M., Alsaeed, Y.H., Nanofluids application for heavy oil recovery, *Soc. Pet. Eng. - SPE Asia Pacific Oil Gas Conf. Exhib. APOGCE*, 2014.
[11] Salem Ragab, A.M., Hannora, A.E., A comparative investigation of nano particle effects for improved oil recovery – Experimental Work, *SPE Kuwait Oil Gas Show Conf.*, Society of Petroleum Engineers, 2015.
[12] Songolzadeh, R., Moghadasi, J., Stabilizing silica nanoparticles in high saline water by using ionic surfactants for wettability alteration application, *Colloid and Polymer Science*, 295, 2017, 145–155.

[13] Yu, W., Xie, H., A review on nanofluids: preparation, stability mechanisms, and applications, *Journal of Nanomaterials*, 2012, 2011, 435873.

[14] Minakov, A.V., Rudyak, V.Ya., Pryazhnikov, M.I., Systematic experimental study of the viscosity of nanofluids, *Heat Transfer Engineering*, 42(12), 2021, 1024-1040.

[15] Minakov, A.V., Pryazhnikov, M.I., Suleymana, Y.N., Meshkova, V.D., Guzei, D.V., Experimental study of nanoparticle size and material effect on the oil wettability characteristics of various rock types, *Journal of Molecular Liquids*, 327, 2021, 114906.

[16] Hirt, C.W., Nichols, B.D., Volume of fluid (VOF) method for the dynamics of free boundaries, *Journal of Computational Physics*, 39(1), 1981, 201-225.

[17] Brackbill, J.U., Kothe, D.B., Zemach, C., A continuum method for modeling surface tension, *Journal of Computational Physics*, 100(2), 1992, 335-354.

[18] Minakov, A.V., Numerical algorithm for moving-boundary fluid dynamics problems and its testing, *Computational Mathematics and Mathematical Physics*, 54(10), 2014, 1560–1570.

[19] Minakov, A.V., Shebeleva, A.A., Yagodnitsyna, A.A., Kovalev, A.V., Bilsky, A.V., Flow Regimes of Viscous Immiscible Liquids in T-Type Microchannels, *Chemical Engineering and Technology*, 42(5), 2019, 1037-1044.

[20] Minakov, A.V., Guzei, D.V., Pryazhnikov, M.I., Filimonov, S.A., Voronenkova, Y.O., 3D pore-scale modeling of nanofluids-enhanced oil recovery, *Petroleum Exploration and Development*, 48(4), 2021, 956-967.

[21] Guzei, D.V., Minakov, A.V., Pryazhnikov, M.I., Dekterev, A.A., Numerical modeling of gas-liquid flows in mini- and microchannels, *Thermophysics and Aeromechanics*, 22, 2015, 61–71.

[22] Abrams, A., Influence of fluid viscosity, interfacial tension, and flow velocity on residual oil saturation left by waterflood, *Society of Petroleum Engineers Journal*, 15(5), 1975, 437-447.

ORCID iD

D.V. Guzei https://orcid.org/0000-0003-2226-1837

A.V. Minakov https://orcid.org/0000-0003-1956-5506

M.I. Pryazhnikov https://orcid.org/0000-0001-9143-7950

S.V. Ivanova https://orcid.org/0000-0002-7803-6471

Publisher's Note Shahid Chamran University of Ahvaz remains neutral with regard to jurisdictional claims in published maps and institutional affiliations.